

## Direct Optical Quantification of Backflow in a $90^\circ$ Twisted Nematic Cell

N. J. Smith and M. D. Tillin

*Sharp Laboratories of Europe Ltd., Edmund Halley Road, Oxford Science Park, Oxford, OX4 4GB, England*

J. R. Sambles

*Thin Film Photonics Group, School of Physics, University of Exeter, Stocker Road, Exeter, EX4 4QL, England*

(Received 10 September 2001; published 7 February 2002)

Optical guided mode observations of the transient director profile (optical tensor distribution) during the relaxation of a  $90^\circ$  twisted nematic cell directly reveals backflow. In the first 6 ms of the relaxation process, after a voltage across the cell is removed, the midplane tilt of the director increases, reaching a maximum value of  $101^\circ$  at 1.4 ms. This increase in midplane tilt is attributed to coupling between fluid flow (backflow) and director reorientation. A  $270^\circ$  twisted state of the opposite handedness to the  $90^\circ$  twisted state found at equilibrium is shown to exist during the backflow period. Good fits of theoretical models with experimentally determined time dependent director profiles yield the viscosity coefficients.

DOI: 10.1103/PhysRevLett.88.088301

PACS numbers: 83.80.Xz

A nematic liquid crystal (LC) flows as easily as any other organic liquid consisting of similar molecules. However, when the state of the molecular alignment in the liquid crystal is considered, the relationship between fluid flow and alignment turns out to be rather complicated. There is a coupling between transitional motion and the orientation of the LC molecules and hence any fluid flow will, in general, disturb the alignment. Conversely, a change in the alignment (e.g., by application of an external electric field) will, in many situations, induce fluid flow. This coupling between fluid flow and director alignment has no isotropic counterpart and is described by the Leslie-Erickson [1,2] hydrodynamic continuum theory of nematic liquid crystals. Numerical methods for solving Leslie-Erickson equations of motion have been used to study the switching dynamics of a  $90^\circ$  twisted nematic (TN) cell [3,4]. This modeling work showed that upon removal of a suitably large externally applied field a temporary reverse of the twist direction occurs during the first few ms. Since the alignment of the nematic is anchored at the boundaries of the cell, the new  $270^\circ$  twist state is of opposite handedness to the equilibrium configuration. In addition, while the  $270^\circ$  twist state is maintained the tilt angle of the director in the middle of the cell actually increases, tipping away from the equilibrium configuration. These intermediate relaxation configurations of reverse twist and increased midplane tilt can occur only when coupling between flow and alignment is included in the numerical simulations.

Experimentally, the above prediction of flow leads to the observed oscillation in the transmission-time curve after a voltage has been removed from a TN cell. This oscillation, the so called “optical bounce,” can be accounted for only if macroscopic fluid flow in planes parallel to the boundaries of the LC cell is taken into consideration [5]. However, until now no direct quantification of the director profile during the relaxation dynamics of a  $90^\circ$  TN has been achieved.

Optical waveguide studies have become a well established tool for use in determining the director profile (optical tensor distribution) in thin liquid crystal films [6–10]. The fully leaky guided mode technique (FLGM) is the latest and most versatile waveguide technique since it can be used to study commercially fabricated LC cells [11]. Recent work has shown that by coupling a convergent beam into waveguide modes dynamic director reorientation processes can be resolved [12]. The work described here employs a convergent beam to excite fully leaky guided modes in a commercially fabricated  $90^\circ$  TN cell, enabling the dynamic evolution of the director profile to be studied with unprecedented accuracy.

The cell investigated comprises two ordinary glass plates ( $n = 1.52$ ) coated with indium tin oxide (ITO) upon which is a rubbed polyimide layer. The rubbing directions on the top and bottom plate are perpendicular, thus inducing a  $90^\circ$  TN state at 0 V. The cell is filled with nematic liquid crystal ZLI-2293 (Merck). Coupling hemispheres are optically matched onto the cell by use of a suitable nonvolatile silicone based oil. This arrangement is shown schematically in Fig. 1.

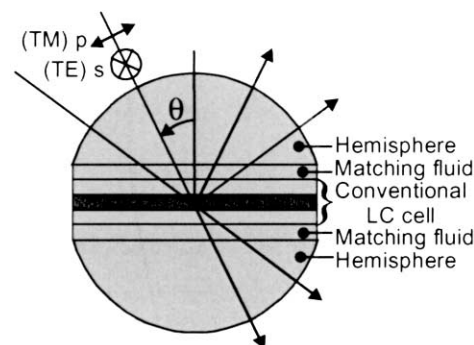


FIG. 1. Hemispheres are used for coupling a convergent beam into and out of fully leaky guided modes that are resonant within the liquid crystal layer of a commercially fabricated cell.

A schematic of the convergent beam arrangement [13] is shown in Fig. 2. The He-Ne laser light (wavelength 632.8 nm) is expanded, polarized, and focused through the hemisphere onto the liquid crystal layer. The reflected and transmitted beams are then captured with a linear CCD array (DALSA SPARK).

A study of the director profile relaxing from a distorted state at 7.0 V rms (10 kHz sine wave) to the equilibrium state at 0 V is undertaken. Relaxation from 7 V was chosen since modeling suggested that upon removal of the voltage the coupling between director reorientation and macroscopic fluid flow is significant for around the first 10 ms. Therefore it should be possible to observe reorientation of the director caused by a macroscopic fluid flow at short time scales.

The general procedure adopted for the TN relaxation study breaks down into two sections: statics and dynamics. In order to characterize the optical parameters of the LC cell (including polyimide and ITO layers), data were taken with no voltage applied to the cell and with 7.0 V rms applied. In total, eight fully leaky data sets were recorded with the cell at 0 and at 7 V. The eight data sets consist of  $R_{pp}$ ,  $R_{ps}$ ,  $R_{sp}$ ,  $R_{ss}$ ,  $T_{pp}$ ,  $T_{ps}$ ,  $T_{sp}$ , and  $T_{ss}$ , where  $R$  and  $T$  correspond to reflection and transmission, respectively; the first subscript indicates the input polarization state and the second subscript indicates the detected polarization state. The optical parameters and director distribution of the cell are obtained by matching experimental reflectivity and transmissivity data with model data generated from multilayer optics theory [14]. Once the optical parameters of the cell have been characterized for these two static situations, analysis of dynamic data recorded as the cell relaxes from 7.0 to 0 V was undertaken.

Switching dynamics of the TN cell were recorded by synchronizing the CCD array to capture data when the voltage across the TN cell was changed. The integration time of the CCD array was 0.2 ms.  $R_{pp}$ ,  $R_{ss}$ ,  $T_{pp}$ ,  $T_{ps}$ ,  $T_{sp}$ , and  $T_{ss}$  signals were all recorded as a function of time.  $R_{ps}$  and  $R_{sp}$  signals were too small to record using a capture time of 0.2 ms. The relaxation process was recorded ten times for each data set and the mean optical response was then calculated. The mean optical response of each data set was then normalized relative to the absolute intensity of

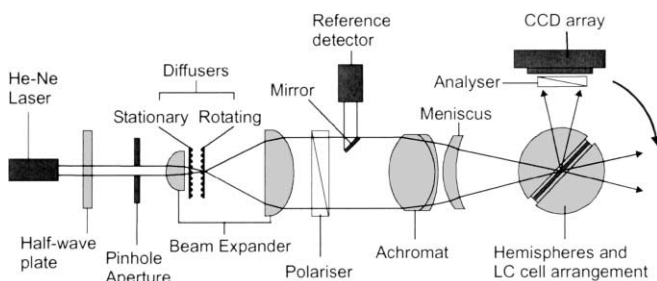


FIG. 2. Schematic representation of bulk optical components. The angular dependent reflectivity and transmissivity data are captured with a CCD array, thus allowing static and dynamic director profiles to be resolved.

the convergent beam. Normalized gray-scale plots showing the time evolution from 0 to 120 ms of the  $R_{pp}$ ,  $R_{ss}$ ,  $T_{pp}$ ,  $T_{ps}$ ,  $T_{sp}$ , and  $T_{ss}$  signals are shown in Fig. 3.

Just before the voltage is removed, the average signal strength of  $T_{pp}$  and  $T_{ps}$  are at a similar level. However, upon removal of the voltage, the  $T_{ps}$  signal increases dramatically in the first ms, indicating that a large amount of direct reorientation occurs. This is intuitive since the elastic torque on the director is greatest in the highly distorted state at 7 V. The average  $T_{pp}$  signal becomes comparable in strength with the average  $T_{ps}$  signal only at long time scales. The  $T_{ss}$  signal behaves in a similar fashion to the  $T_{pp}$  signal over the 120 ms time scale. The rate of change of the  $T_{sp}$  signal is much slower than the  $T_{ps}$  signal, with little evolution occurring in the first 20 ms time period. The  $R_{pp}$  signal changes rapidly in intensity in the first few ms after the voltage has been removed and clearly all modes shift to lower angles. At around 40 ms the mode at around  $75^\circ$  bifurcates, and at 50 ms the mode at  $72^\circ$  also bifurcates. These bifurcations provide interesting optical features to which to fit model theory. The  $R_{ss}$  signal is

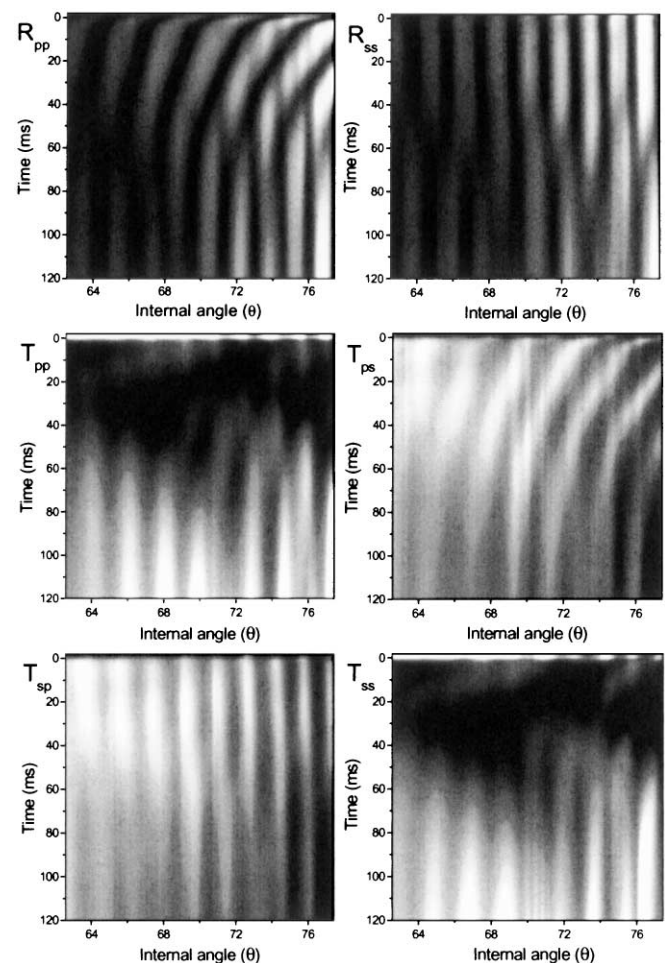


FIG. 3. Gray-scale plots showing the time evolution of the  $R_{pp}$ ,  $R_{ss}$ ,  $T_{pp}$ ,  $T_{ps}$ ,  $T_{sp}$ , and  $T_{ss}$  signals as the TN cell relaxes from 7.0 to 0 V over the first 120 ms. High optical intensity is represented in white.

strange in the fact that it barely changes for the first 50 ms of the relaxation process. This is rather counterintuitive, as the director profile will have undergone major reorientation during this time period. However, the sensitivity of fully guided modes to changes in the director profile depends on the director profile itself at any instant in time. Consequently, different fully leaky guided modes become particularly sensitive to the transient director profile for different time periods of the dynamic process. Clearly the  $R_{ss}$  signal is significantly different after 120 ms, the majority of these changes occurring in the time period between 50 and 90 ms.

In order to quantify the director profile at particular stages of the relaxation process, the experimental data at individual times must be fitted with model data produced by the multilayer optics theory. Fits were obtained by using a minimization routine to find a solution that gives a least sum of squares between the experimental data and theoretical model. For many of the fits, a variety of functional forms were used to describe the twist and tilt profiles to ensure that the parameter space had been fully explored before a least squares fit was chosen. Sample fits for the  $T_{pp}$  and  $T_{ps}$  signals are shown in Fig. 4, for the transient optical signals at various times. Fits to the  $R_{pp}$ ,  $R_{ss}$ ,  $T_{ss}$ ,

and  $T_{sp}$  signals are of similar quality. The fits illustrated start with the static case at 7 V ( $t = 0$  ms) followed by the transient signals for the times 1, 4, 16, and 70 ms after the removal of the voltage and concludes with the static case at 0 V ( $t = \infty$ ). Alongside each fit is the twist and tilt profile that was used in order to obtain the fit.

Initially at  $t = 0$  ms, the midplane tilt of the director is almost  $90^\circ$  and consequently the majority of the  $90^\circ$  left-handed twist occurs in the center of the cell. The actual twist through the cell is measured to be  $88^\circ \pm 1^\circ$ , thus causing a handedness preference for the twist. Upon removal of the voltage, the largest elastic torque on the director occurs in the vicinity of the cell walls. Reorientation of the director is therefore fastest in these regions of high elastic torque and has the largest fluid flow associated with it. The fluid flow, or “backflow,” couples to the director in the center of the cell in such a way that the midplane tilt actually increases. When the midplane tilt reaches a value of exactly  $90^\circ$ , the twist in the system has effectively become undefined in the center of the cell. As the midplane tilt of the director continues to increase beyond  $90^\circ$  the twist is once again defined but now exists of opposite handedness, twisting through a total of  $270^\circ$  in order to satisfy the boundary conditions of the cell. The transition from the initial  $90^\circ$  to the  $270^\circ$  twist state occurs over time scales too short to quantify in this experiment, i.e.,  $\ll 0.2$  ms after the removal of the voltage. The dynamic fit at 1 ms shows a  $270^\circ$  twist state occurring in the opposite direction to the  $90^\circ$  twist that existed in the static state at  $t = 0$  ms. The midplane tilt angle is found to increase to a maximum value of  $101^\circ$  at 1.4 ms. As the relaxation process continues, the backflow decreases and the midplane tilt angle starts to decrease. After about 6 ms, the midplane tilt is observed to have returned to  $90^\circ$  and again the twist becomes undefined in the middle of the cell. As the midplane tilt decreases below  $90^\circ$ , a  $90^\circ$  left-handed twist state is once again found within the cell and this remains for the remainder of the relaxation process. The functional form of the twist state evolves asymptotically to a linear profile at around 70 ms into the relaxation process. However, the tilt profile at 70 ms is still far from its equilibrium state, the midplane tilt taking a value of around  $22^\circ$  at this point in the relaxation process.

Taking published values for the viscosity coefficients [15], the elastic constants and dielectric anisotropy of ZLI-2293, the variation of midplane tilt was modeled theoretically using commercially available software (DIMOS LCD workbench and toolset software; produced by Autronic Melchers GmbH). The variation of the midplane tilt value with respect to time determined from experiment was then compared with this modeling, the results of which are shown in Fig. 5. For some of the fitted time slots, two or more values of midplane tilt have been given in Fig. 5. The reason for this is that different functional forms for the tilt profile were investigated at many of the time slots. Sometimes two different functional forms gave fits of very similar quality and therefore the range of these multivalued

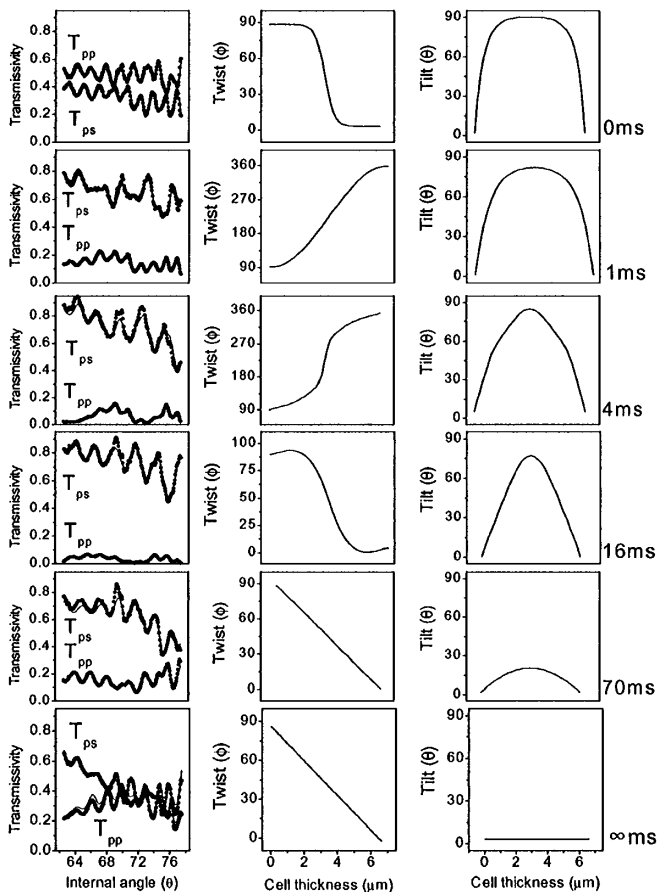


FIG. 4. A selection of fits at various times to the transient optical signals  $T_{pp}$  and  $T_{ps}$ , and the corresponding director profile used to obtain fits to the experimental data.

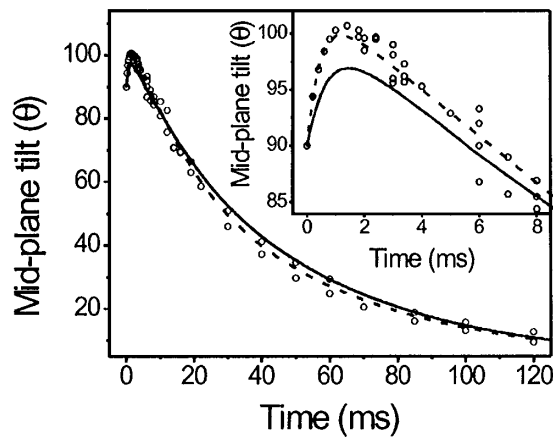


FIG. 5. The variation of midplane tilt in the TN cells with time relaxing from 7 V. The relaxation process from 0–8 ms is inset to highlight the backflow region. The solid line represents the modeled theoretical response using previously published viscosity values, the dashed line represents the modeled theoretical response using a modified set of viscosity values, and the circles are the experimentally determined values of the midplane tilt.

points in time is representative of the experimental error in midplane tilt. Figure 5 demonstrates that the general trend of the experimentally determined midplane tilt (circles) agrees reasonably well with the theoretically modeled relaxation (solid line). However, noticeable differences occur in the backflow region (times  $< 6$  ms) where the midplane tilt goes beyond  $90^\circ$ . In the backflow region, although the positions of the maximum midplane tilts agree, theory suggests that the maximum value of the midplane tilt is  $97^\circ$  whereas the maximum measured value appears to be  $101^\circ$ .

In order to obtain better agreement between the theoretical and experimentally determined temporal evolution of the midplane tilt, the influence of the viscosity coefficients on the relaxation process were investigated. A modified set of viscosity coefficients was found to model the experimentally determined relaxation process more accurately, the results of which are shown in Fig. 5 (dashed line). The viscosity values used to obtain the improved fit in Fig. 5 are  $\eta_1 = 0.16$  Pa s,  $\eta_2 = 0.01$  Pa s,  $\eta_3 = 0.03$  Pa s,  $\eta_{12} = -0.1$  Pa s, and  $\gamma_1 = 0.155$  Pa s. Good agreement in the backflow region ( $t < 6$  ms) using the modified set of viscosity coefficients is now observed and is significantly better than that obtained by modeling the relaxation process with the published viscosity values. The value of  $(\eta_1 - \eta_2)/\gamma_1$  is within 10% of unity and has a value of 0.97 for the modified set of viscosity coefficients, thus agreeing with predictions based on ellipsoidal molecules [16]. In addition, the general rule derived from microscopic models [17] that for nematic liquid crystals,  $\eta_1 > \gamma_1 > \eta_3 > \eta_2$ , is also adhered to. None of the thermodynamic inequalities are violated using this new set of viscosity coefficients.

In conclusion, the convergent beam has been used to excite fully leaky guided modes in a commercially fabricated,  $90^\circ$  twisted nematic cell filled with the material ZLI-2293. The temporal variation of the director profile has been resolved with a resolution of 0.2 ms as the cell relaxed from a distorted state at 7 V to an equilibrium state at 0 V. In order to fit the dynamic optical data, a “backflow region” was identified for short time scales, which was predicted by Berreman [3] and van Doorn [4]. In the backflow region, the midplane tilt of the director was found to increase to a maximum value of  $101^\circ$  after the voltage had been removed for 1.4 ms. The midplane tilt remains larger than  $90^\circ$  for times less than 6 ms. A  $270^\circ$  twisted state of opposite handedness to the  $90^\circ$  twisted state that occurs at 0 V was found to occur during the backflow region. By fitting theoretically predicted temporal midplane tilt variation to that determined from experiment enabled the viscosity coefficients of ZLI-2293 to be determined.

The authors wish to thank EPSRC and Sharp Laboratories of Europe, Ltd. for the financial support of this work and The Liquid Crystal Research Center, Tsinghua University, Beijing for providing the LC cells.

- 
- [1] F. M. Leslie, *Arch. Ration. Mech. Anal.* **28**, 265 (1968).
  - [2] J. L. Ericksen, *Trans. Soc. Rheol.* **5**, 23 (1961).
  - [3] D. W. Berreman, *J. Appl. Phys.* **46**, 3746 (1975).
  - [4] C. Z. van Doorn, *J. Appl. Phys.* **46**, 3738 (1975).
  - [5] C. Z. van Doorn, C. J. Gerritsmas, and P. van Zanten, *Phys. Lett. A* **48**, 263 (1974).
  - [6] F. Yang, G. W. Bradberry, and J. R. Sambles, *Phys. Rev. E* **53**, 674 (1996).
  - [7] S. J. Elston and J. R. Sambles, *Appl. Phys. Lett.* **55**, 1661 (1989).
  - [8] S. Ito, F. Kremer, T. Fisher, and W. Knoll, *Mol. Cryst. Liq. Cryst.* **264**, 99 (1995).
  - [9] G. J. Sprokel, R. Santo, and J. D. Swalen, *Mol. Cryst. Liq. Cryst.* **68**, 29 (1981).
  - [10] M. Mitsuishi, S. Ito, and M. Yamamoto, *J. Appl. Phys.* **81**, 1135 (1997).
  - [11] F. Yang and J. R. Sambles, *J. Opt. Soc. Am. B* **16**, 488 (1999).
  - [12] N. J. Smith and J. R. Sambles, *Appl. Phys. Lett.* **77**, 2632 (2000).
  - [13] N. J. Smith and J. R. Sambles, *J. Appl. Phys.* **85**, 3984 (1999).
  - [14] D. Y. K. Ko and J. R. Sambles, *J. Opt. Soc. Am. A* **5**, 1863 (1988).
  - [15] D. Armitage and J. Larimer, in *SID 96 Applications Digest* (Society for Information Display, Santa Ana, CA, 1996), p. 584.
  - [16] H. Walton and M. J. Towler, *Liq. Cryst.* **27**, 1329 (2000).
  - [17] H. Ehrentraut and S. Hess, *Phys. Rev. E* **51**, 2203 (1995).